Pergamon

Comput. Biol. Med. Vol. 26, No. 2, pp. 143–159, 1996

Printed in Great Britain
0010-4825/96 $15.00 + 0.00

0010-4825(95)00049-6

SIGNAL PROCESSING METHODS FOR PULSE OXIMETRY

T. L. RUSCH,* R. SANKAR† and J. E. SCHARF‡

*Marshfield Medical Research Foundation, Center for Medical Genetics, Marshfield, WI 54449, U.S.A.; †Department of Electrical Engineering, University of South Florida, Tampa, FL 33620, U.S.A.; and ‡Department of Anesthesiology, University of South Florida, Tampa, FL 36620, U.S.A.

(*Received* 31 *May* 1995; *received in revised form* 10 *October* 1995)

Abstract—Current signal processing technology has driven many advances in almost every aspect of life, including medical applications. It follows that applying signal processing techniques to pulse oximetry could also provide major improvements. This research was designed to identify and implement one or more techniques that could improve pulse oximetry oxygen saturation (SpO_2) measurements. The hypothesis was that frequency domain analysis could more easily extract the cardiac rate and amplitude of interest from the time domain signal. The focus was on the digital signal processing algorithms that had potential to improve pulse oximetry readings, and then test those algorithms. This was accomplished using the Fast Fourier Transform (FFT) and the Discrete Cosine Transform (DCT). The results indicate that the FFT and DCT computation of oxygen saturation were as accurate without averaging, as weighted moving average (WMA) algorithms currently being used, and directly indicate when erroneous calculations occur.

Pulse oximetry Oxygen saturation (SpO_2) computation Spectral analysis Signal processing

NOMENCLATURE

α	extinction coefficient
μ	attenuation coefficient
ASA	American Society of Anesthesiologists
C	concentration
DCT	Discrete Cosine Transform
DFT	Discrete Fourier Transform
DHT	Discrete Hartley Transform
DPP	digital photoplethysmogram
DST	Discrete Sine Transform
FFT	Fast Fourier Transform
Hb	hemoglobin
I_{trans}	transmitted light intensity
KL	Karhunen–Loeve
LED	Light Emitting Diode
N	transform size
O_2Hb	oxygenated hemoglobin or oxyhemoglobin
PaO_2	partial pressure of oxygen in hemoglobin
R	normalized ratio of red to infrared intensity
RSFFT	real input split radix Fast Fourier Transform
SIDS	sudden infant death syndrome
SpO_2	pulse oximetry arterial oxygen saturation
SRFFT	split radix Fast Fourier Transform

This research work was supported in part by a grant from Group Technologies, Inc.

SVD	Singular Valve Decomposition
VLSI	Very Large Scale Integration
WMA	weighted moving average

INTRODUCTION

"For life, nothing is more important than oxygen supply. Thus one might argue that nothing is more important to monitor during the care of the unconscious or disabled patient than the color of the arterial saturation" [1]. Here starts the justification for pursuing an advanced design for a portable pulse oximeter. The measurement of the percent oxygen saturation in hemoglobin, called oximetry, has been performed since the 1930s. It took 60 years for pulse oximetry to become a standard piece of equipment in operating rooms, critical care units and emergency health care. However, because of cost and usefulness, the future use in other areas is limited. This provides an incentive to improve on current techniques, and design a more accurate, stable, and cost effective portable pulse oximeter.

Pulse oximetry has become an accepted tool for saving lives during surgery, however, many other applications can benefit from its use. Many research papers have addressed the issue of pulse oximetry accuracy and applying pulse oximetry to new areas. Some of the applications are listed in Table 1 from a review article [2]. As can be seen the papers reviewed show a wide range of use. Additional uses have included high altitude oxygen measurement, underwater diving measurements, and home health care monitoring. The biggest disadvantage of using current pulse oximeters in these applications is the portability and reliability of the unit.

The main motivation to develop a portable oximeter was based on the potential benefits of such a unit. Current pulse oximeters are relatively expensive, have inaccuracies, and are not very portable. New pulse oximeters on the market have made progress on portability. However, a miniature 3×3 inch model, with no external wire for data acquisition, has never been developed. There also exist many applications beyond the current use of pulse oximetry, for example, non intensive care monitoring, outpatient surgery, medical research, home health care and monitoring, dentistry anesthesia monitoring, sudden infant death syndrome (SIDS) monitoring, recreational sports like scuba diving or mountain climbing, and many others. All of these areas could benefit from a less expensive, more accurate, and more portable pulse oximeter. In addition, pulse oximetry has already been beneficial. A two part study on pulse oximetry shows a 19-fold increase in the diagnosis of hypoxemia when using oximetry as compared to not using oximetry [3].

Current pulse oximeters use a weighted moving average techniques to compute oxygen saturation (SpO_2) values. This method has many limitations including susceptibility to motion artifact, background light, and low perfusion errors. The goal for developing an

Table 1. Pulse oximeter use reported by number of publications

Subject	Number of papers
Endoscopy	26
Postoperative recovery	22
Neonatal intensive care unit	21
Oral surgery and dentistry	14
Airway management	13
Sleep studies	13
Hypotension, poor perfusion	12
Premedication	11
Pediatric anesthesia	10
Transport	10
Emergency	9
Chronic obstructive pulmonary disease, lung disease	8
Adequacy of circulation test	8
Anesthesia, adult	8

alternate method for pulse oximetry was to overcome these limitations. Spectral analysis was identified as having a good potential for improving SpO_2 computation, and preliminary test results agreed with this hypothesis.

The main objective and the resulting contributions of this research addressed two aspects of designing a portable pulse oximeter. The first was to show the use of spectral analysis to calculate SpO_2 values is a practical solution. The second was to identify alternate methods of computing these values that provided acceptable results, which includes the Fast Fourier Transform (FFT), and the Discrete Cosine Transform (DCT).

This paper begins by presenting a brief history of pulse oximetry, theories behind pulse oximetry, computation methods, and limitations of pulse oximetry. The paper concludes with a discussion of the computation results.

PULSE OXIMETRY THEORY AND COMPUTATION

History of oximetry

The original development of the oximeter did not occur at one specific time in history, which is the case with most developments. Early oximeters used light transmission to measure oxygenation, but they used invasive samples [4]. Non-invasive measurements are always preferred over invasive measurements, because invasive measurements increase risk of infection, and usually mean some delay between the time of acquisition and the time results are available. Matthes and Millikan recorded the earliest non-invasive reading around 1935, and Glen Millikan introduced the term oximetry in 1942. The early development of pulse oximeters was performed for military aviation during World War II [1]. After a long period with little change in pulse oximetry, the clinical use and benefits were recognized. On 1 January 1990, the American Society of Anesthesiologists (ASA) made the intraoperative monitoring with pulse oximetry a standard [5]. Despite the acceptance of pulse oximetry and its benefits, there still has been little change in pulse oximetry techniques.

Oximetry

Oximetry is the measurement of the percent saturation of oxygen in hemoglobin. This measurement is directly correlated to the partial pressure of oxygen in hemoglobin (PaO_2). The partial pressure of oxygen in hemoglobin determines how well oxygen is delivered to the bodies cell tissue. If oxygen is not delivered properly, cell tissue will be damaged. In the same respect the percent oxygen saturation is a means of identifying how well oxygen is delivered to the bodies cell tissue. The basic concept in oximetry is to transmit light through a blood sample, and the blood will absorb a determined amount of light depending on the concentration of oxygenated and deoxygenated hemoglobin. The assumption is that blood is composed of only oxygenated and deoxygenated hemoglobin. This is a very simplified description, but it is the basis for oximetry measurements.

The first oximeters used invasively drawn samples [4]. For *in vivo* measurements the path length for the light is constant. For pulse oximetry, however, the light illuminates both arterial and venous blood and the light must transverse all tissue between light source and receiver. Figure 1 represents the light path, and indicates a variable (AC) path length as well as a constant (DC) path length [6]. This points out that the assumption of only oxygenated and deoxygenated hemoglobin is in error.

Light absorption in hemoglobin

Pulse oximetry is based on the transmission, absorption, and dispersion of light as it passes through hemoglobin. The transmission of light through a substance is determined by Beers–Lambert law, also referred to as Beer's law [7]. The transmitted light intensity (I_{trans}) is given as

$$I_{trans} = I_{in}\, e^{-DC\alpha}, \tag{1}$$

where D is the distance the light travels through the substance, C is the concentration of the solution and alpha (α) is the extinction coefficient.

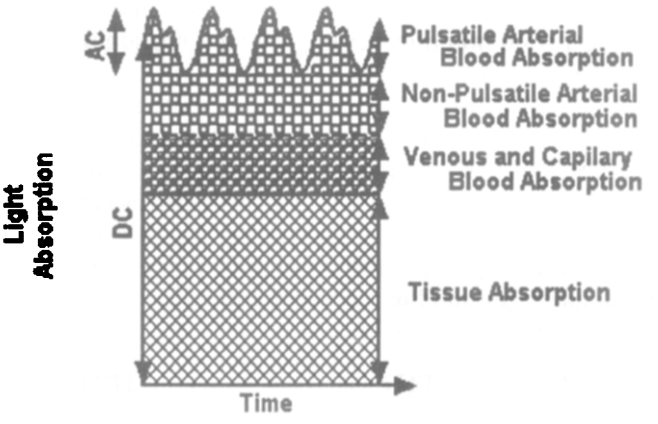

Fig. 1. Light path length versus time [4].

For oximetry applications, hemoglobin is assumed to be composed of two substances, oxygenated hemoglobin or oxyhemoglobin (O_2Hb) and deoxygenated or reduced hemoglobin (Hb). If two light wavelengths are used and the two substances have different extinction coefficients (α), or equivalently attenuation coefficients (μ), then the percentage of each substance can be calculated. If the light travels through a constant distance, the arterial oxygen saturation (SaO_2) is given as

$$S_aO_2 = \frac{c_{ox}}{c_{ox} + c_{Dox}}. \tag{2}$$

The concentration of oxyhemoglobin is given by c_{ox} and the concentration of deoxygenated hemoglobin is given by c_{Dox} [8]. This formula however, must be adjusted for other contents in the blood which influence measurements.

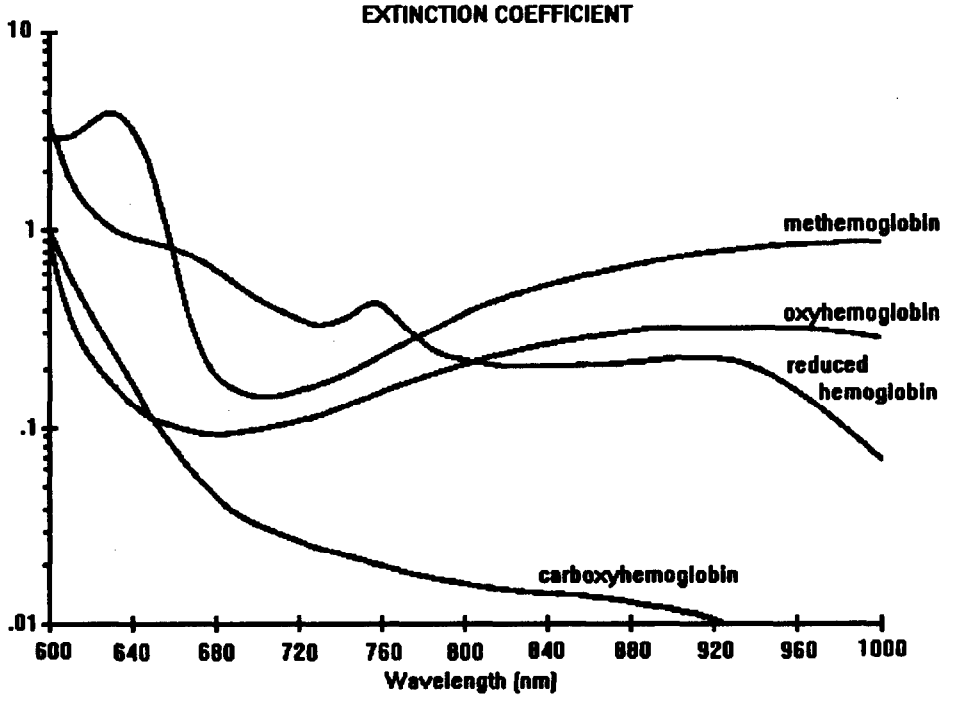

Fig. 2. Extinction curve for oxyhemoglobin, reduced hemoglobin, methemoglobin, and carboxyhemoglobin [9].

The extinction coefficients of hemoglobin are well documented and Fig. 2 charts the extinction coefficients for oxyhemoglobin and reduced hemoglobin [6]. The two wavelengths of light yielding the best results are the red (660nm) and infrared (940nm) wavelengths. Red has the largest difference between the two extinction curves, and infrared has maximal difference after the two extinction curves cross. At 805nm the two extinction curves cross and it is called the isobestic point. At the isobestic wavelength the absorption coefficient for both oxyhemoglobin and reduced hemoglobin is the same and the light attenuation is independent of oxygen saturation.

SpO_2 computation

To calculate the pulse oximetry digital photoplethysmogram (DPP) oxygen saturation (SpO_2), two equations are used. An example of a DPP signal is shown in Fig. 3 and the AC and DC DPP components are identified. The first step is to use the red and infrared time signal to calculate an R value [6]. The R value is the normalized ratio of the red to infrared transmitted light intensity. The normalized value is obtained by measuring the AC DPP component and dividing by the DC DPP component. The R value is given as

$$R = \frac{AC_{red}/DC_{red}}{AC_{infrared}/DC_{infrared}}. \tag{3}$$

The R value for two specific light wavelengths can be plotted against a measured SaO_2 value, as shown in Fig. 4 [6]. A linear approximation can then be used to calculate a SpO_2 value. The empirical linear approximation for Fig. 4 is given as

$$SpO_2 = 110 - 25R. \tag{4}$$

The empirical approximation is used to correct for errors in the measured values. The errors are a result of assuming the presence of only two substances in the light path. This introduces one of the limitations of pulse oximetry.

Pulse oximetry limitations

There are many areas where pulse oximetry has limitations, and some of these limitations will be addressed. One limitation was already mentioned, and that is the assumption of only two substances in hemoglobin. In addition to oxyhemoglobin and reduced hemoglobin, several other substances including methemoglobin and carboxyhemoglobin exist and must be considered. Figure 2 shows the extinction plots of the four substances [9]. To account for the additional substances properly, additional light sources must be used. However, for most measurements the percentage of these substances is small enough not to effect the pulse oximetry measurements. There are cases in emergency care when these substances may be present and do affect readings. At present the user must be aware of the limitations and not use the pulse oximetry reading if the person has any of the additional substances. In most current applications this is not

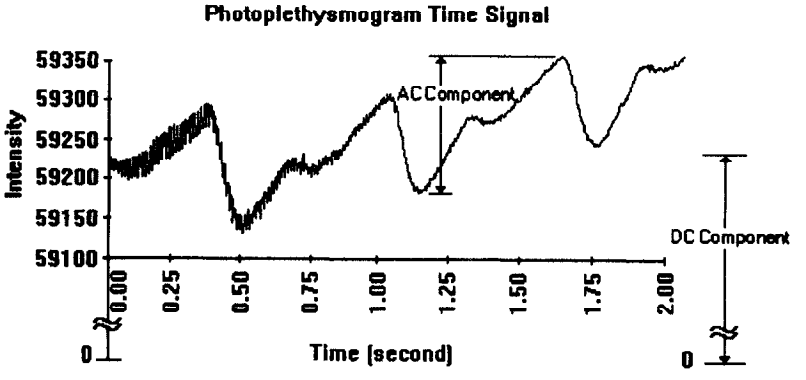

Fig. 3. Pulse oximetry signal with pulsatile component.

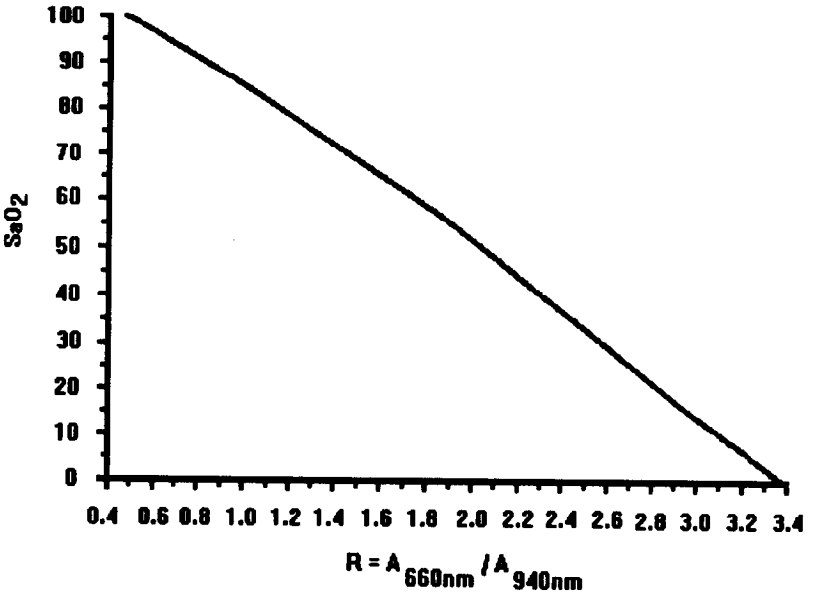

Fig. 4. SaO_2 value vs R value [6].

a problem, but as pulse oximeters are used for more applications, the incorrect application becomes more of a problem. The solution is to use additional light sources to calculate additional substance concentrations [10,11]. The first pulse oximeters tested, used multiple wavelength light source and could easily be implemented in new measurement techniques.

A second limitation of pulse oximetry is background light. Because pulse oximetry currently uses transmitted light, the photodiode receiver is susceptible to ambient light, either indoor lighting or sun light, and phototherapy lights [2]. To correct for this problem three methods can be exploited. These methods include shielding, using a third light measurement to subtract ambient light, or use an alternate measurement technique. Additional shielding can be used, but it adds bulk and expense. Measuring a third sample while cycling the red and infrared light emitting diodes (LEDs) adds a small amount of complexity, but the background signal must be subtracted from the LED signal. If analog processing is used, subtraction adds to the complexity of the signal processing. If digital processing with a microprocessor is used, the subtraction means adding only one operation. An alternate technique to consider is a reflectance probe measurement. Because reflectance probes can be placed flat on the measurement area, they provide better shielding than a probe placed across a finger.

Another limitation is called low perfusion [2]. Pulse oximetry is based on having a pulsatile signal. If the pulsatile signal is small compared to the DC signal, usually 1 count in 1000, the R value calculation becomes inaccurate. There are two reasons for the inaccuracy, round off error and resolution. The round off error can be compensated for by using more precision during the R value calculations. Resolution can be improved by using brighter photodiodes and more accurate A/D converters, or by using a different measurement technique. If more accurate photodiodes and A/D converters are used, the cost of the system is increased. This research project used an alternate technique. A Texas Instruments TSL220, and improved TSL230, light to frequency converter was used. The light to frequency converter does not require an A/D converter and has a wide dynamic range. The assumption based on empiricism was that the TSL230 would provide better resolution and lower noise than a photodiode and A/D converter combination.

A difficult limitation to eliminate is motion artifact and autonomic nervous system response [12–14]. Whenever there is an automatic nervous system action, there is a transition or movement in the pulse oximetry signal. Figure 5 shows an example of motion artifact. The most common technique to correct for motion artifact is averaging

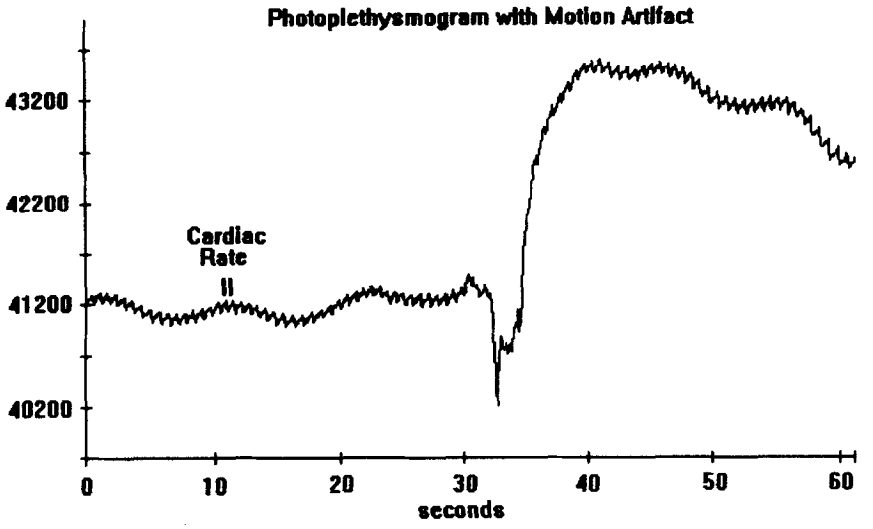

Fig. 5. Example of motion artifact.

of consecutive measurements. This approach works, but it slows the response time and lengthens the processing time. Another improvement would be to identify and eliminate inaccurate readings. This approach, however, is difficult to implement.

Another limitation due to hardware implementation is the wavelengths of the LEDs used must be known exactly. The assumption is each LED is at a single known wavelength, however, LEDs produce a band of wavelengths. In addition LEDs are specified with a range of wavelengths. If a 660nm LED is specified, the center wavelength can be expected to range ± 15nm and have a bandwidth of 20nm. The current method to correct for the LED shift is to measure the LED output at manufacturing time and compensate with the appropriate linear equation. The measured results provide an accuracy within ±2.65 one standard deviation. However, the disadvantage is an increased manufacturing cost. An alternate solution is to test LEDs and use only those within a small wavelength range. This approach increases component cost, which also increases the final cost of the pulse oximeter.

SIGNAL PROCESSING METHODS

There are three steps in this analysis of alternate transforms: The FFT optimization, the FFT and DCT processing results, and the post processing analysis. The optimization analysis was performed on the FFT by fixing all the variables except one, and calculating the FFT for that range. The sample frequency ranged from the standard 240 Hz down to 7.5 Hz, the number of samples ranged from 2048 to 16 points, and the time interval ranged from 0.03 to 34.13 s. The FFT analysis was used to select a more optimum range of transforms for further analysis of the FFT and DCT.

The results were compared to a bench mark transform of a 1024 point transform, sampled at 240 Hz. A 1024 point transform was previously used to accurately calculate SpO_2 values [15]. After the optimization three transform sizes of 32, 64 and 128 were processed at frequencies of 7.5, 15 and 30 Hz. Two transforms were selected for further analysis, the DFT and DCT. The data were processed using MATLAB software with programs developed to systematically process the transforms. The data were tabulated using Microsoft EXCEL software.

The bias was calculated as the mean difference from stable Co-oximeter readings. The precision was calculated as one standard deviation from the mean. The sampled data used for analysis were previously collected after institutional review board approval, and informed written consent from volunteers breathing normoxic and hypoxic gas mixtures. Arterial blood samples were drawn from a radial arterial line and processed with an IL-482 Co-oximeter. Both red and infrared DPPs were recorded for 60 s intervals at

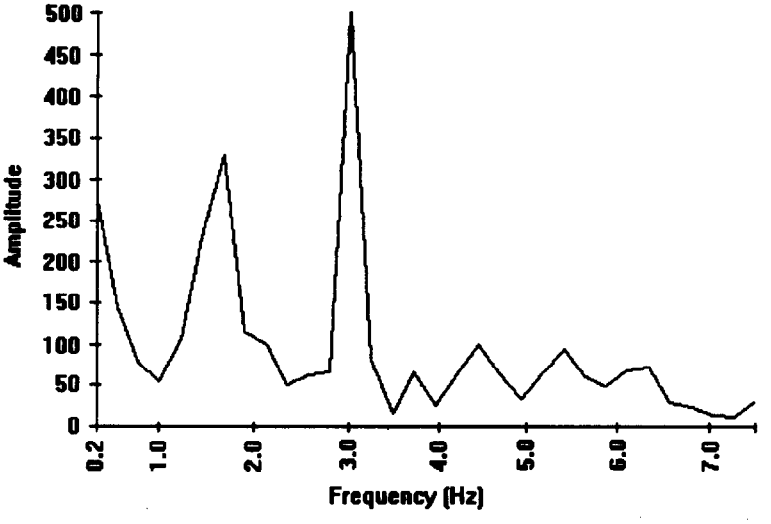

Fig. 6. Sample FFT output.

arterial hemoglobin oxygen saturations of 96.9%, 94.6%, 90.8%, 87.5%, 86.8% and 77.3%.

SpO_2 values were calculated using the DC component amplitude and the AC cardiac frequency amplitude. In the frequency domain transform, the DC component was selected as the zero frequency component amplitude and the AC cardiac frequency component amplitude was selected as the highest spectral line between 1 and 2 Hz. The range of cardiac frequencies corresponds to a cardiac rate of 60–120 beats per minute. The cardiac frequency selection for the FFT is shown in Figs 6 and 7 for the DCT. After identifying the AC and DC components, equations (3) and (4) were used to calculate an SpO_2 value.

The final analysis included post processing of the FFT and DCT computation to identify additional improvements in accuracy. Several techniques were used including median filtering, standard averaging, and point elimination of known bad data computations. In order to perform averaging and not increase the response time of the measurements, overlap processing was used. The results of averaging were compared to the original computations. Several techniques were used including, standard averaging, median averaging and point elimination. Eliminating points was based on the maximum date of desaturation. From previous studies, a nominal deviation of two percent change

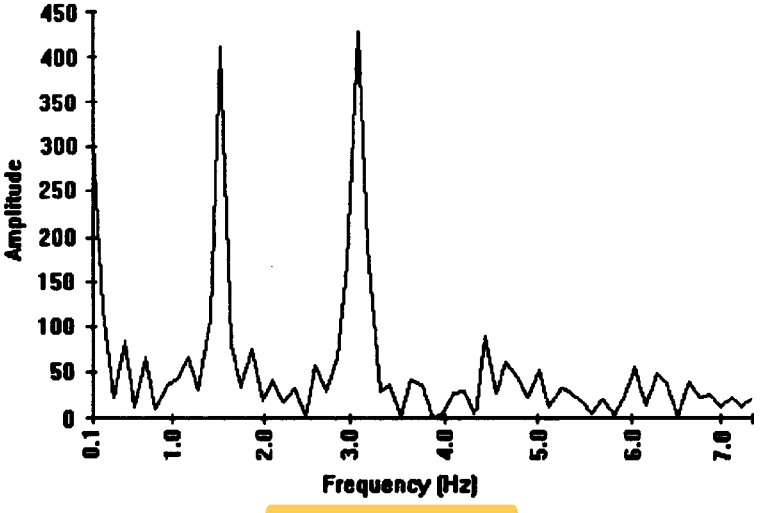

Fig. 7. Sample DCT output.

Table 2. Precision and bias of FFT with all samples

Frequency	Points	16	32	64	128	256	512	1024	2048
240 Hz	Bias	—	—	—	—	—	0.37	0.54	0.36
	Precision	—	—	—	—	—	3.40	3.73	3.99
120 Hz	Bias	—	—	—	—	0.37	0.54	0.36	−0.42
	Precision	—	—	—	—	3.41	3.73	4.00	5.43
60 Hz	Bias	—	—	—	0.36	0.54	0.35	−0.38	−2.73
	Precision	—	—	—	3.42	3.73	4.02	5.44	10.15
30 Hz	Bias	—	—	0.29	0.53	0.25	−0.28	−2.67	−3.76
	Precision	—	—	3.45	3.67	4.01	5.50	10.12	10.69
15 Hz	Bias	—	0.24	0.50	0.15	−0.17	−2.73	−38.1	—
	Precision	—	3.48	3.67	4.01	5.56	10.49	10.91	—
7.5 Hz	Bias	0.21	0.32	−0.15	0.09	−2.65	−4.04	—	—
	Precision	4.02	3.91	4.43	5.81	10.11	11.22	—	—

Table 3. Precision and bias of FFT with 100 samples

Frequency	Points	16	32	64	128	256	512	1024	2048
240 Hz	Bias	—	—	—	—	—	0.14	0.46	—
	Precision	—	—	—	—	—	2.99	3.76	—
120 Hz	Bias	—	—	—	—	0.13	0.46	—	—
	Precision	—	—	—	—	3.00	3.76	—	—
60 Hz	Bias	—	—	—	0.11	0.46	—	—	—
	Precision	—	—	—	3.01	3.76	—	—	—
30 Hz	Bias	—	—	0.05	0.47	—	—	—	—
	Precision	—	—	2.95	3.71	—	—	—	—
15 Hz	Bias	—	−0.01	0.44	—	—	—	—	—
	Std Dev	—	2.95	3.70	—	—	—	—	—
7.5 Hz	Bias	0.31	0.33	—	—	—	—	—	—
	Precision	3.33	3.98	—	—	—	—	—	—

in a 1 s interval was identified as a maximum [16–18]. If a calculated SpO_2 value deviated more than 2 per cent from the stable SpO_2 values previously calculated, the value was eliminated from the data sequence.

SIGNAL PROCESSING RESULTS

The bias and precision results for the FFT optimization are listed in Tables 2 and 3. Table 2 lists the bias and precision using all the intervals processed. Table 3 is the bias

Table 4. FFT mean and standard deviation

Frequency	Points	32	64	128
30 Hz	Bias	—	−0.28	0.23
	Precision	—	2.71	3.64
15 Hz	Bias	0.18	−0.18	—
	Precision	2.64	2.88	—
7.5 Hz	Bias	0.05	—	—
	Precision	3.03	—	—

Table 5. DCT mean and standard deviation

Frequency	Points	32	64	128
30 Hz	Bias	—	0.10	0.29
	Precision	—	2.28	2.11
15 Hz	Bias	0.52	0.49	—
	Precision	2.01	1.72	—
7.5 Hz	Bias	−0.83	—	—
	Precision	5.15	—	—

and precision from exactly 100 data sets. Table 2 was used as a reference and Table 3 was used to identify that the bias and precision was retained for a transform size as low as 32 points and sampling at 7.5 Hz. The bias and precision continued to improve down to 15 Hz and started to degrade at 7.5 Hz.

The reduced range identified in the FFT optimization analysis was used to compare the computations of the FFT and DCT. The analysis bias and precision results using 100 data sets are listed in Tables 4 and 5. The computations again indicate tht the FFT and DCT provide accurate results down to a transform size of 32 points and sample rate of 7.5 Hz.

The final analysis was post processing of the FFT and DCT computations. Averaging was used in combination with overlap processing and the results are listed in Table 6. Table 6 indicates that all methods provide some improvement. Using more averages continued to improve the precision, however the return was increasingly marginal and the response time continued to increase. Table 6 also indicates the best results were obtained by using both point elimination and standard averaging, and the DCT resulted in a bias and precision of 1.09% and 1.63%, respectively. The bias and precision's calculated are well within the ±2.65% precision of current pulse oximeters on the market.

DISCUSSION OF RESULTS

Alternate transforms

The original intent of this research was to develop a Fast Fourier Transform (FFT) technique for improving pulse oximetry oxygen saturation (SpO_2) computation. However as work progressed it became increasingly clear that alternate transforms should be considered resulting in an expanded search for alternate transforms. A broad search to identify alternate transforms which had the potential to improve pulse oximeter limitations was performed.

The Fast Fourier Transform was the first transform selected for spectral analysis, where the time signal is transformed into the frequency domain. This approach allows the cardiac frequency and amplitude to be directly selected from the transform [19]. The pulse oximetry signal, like the electrocardiogram, is a non-stationary signal, because the cardiac rate varies over time. The FFT is based on the assumption of a stationary signal. As the signal deviates from a stationary signal the calculated error increases in the frequency domain. Transforms that do not require stationarity would not be affected by the variations in heart rate like the FFT. Therefore a search for alternate transforms less

Table 6. Comparison of bias and precision using averaging

A	B	C	Algorithm WMA	Bias 0.2–13%	Precision 1.5–16%
			FFT	−0.47%	3.40%
√			FFT	0.18%	4.01%
√	√		FFT Median	0.14%	3.45%
√	√		FFT 4 Point	0.27%	2.62%
√	√		FFT 8 Point	0.23%	2.87%
√		√	FFT	1.01%	2.84%
√	√	√	FFT 4 Point	0.99%	2.38%
			DCT	0.29%	2.08%
√			DCT	0.62%	2.59%
√	√		DCT Median	0.67%	2.16%
√	√		DCT 4 Point	0.76%	1.93%
√	√		DCT 8 Point	0.70%	2.11%
		√	DCT	0.90%	1.85%
√	√	√	DCT 4 Point	1.09%	1.63%

A—Overlap processing
B—Average processing
C—Elimination processing

dependent on stationarity were sought. The following discussion presents the selection of two transforms to be tested against weighted moving average (WMA) algorithms.

Basic transforms

Many transforms have been used in processing time domain signals to identify many different characteristics. Each transform provides better information for a specific task. Some of the transforms reviewed are listed in Table 7, along with a specific application which they are better suited [20, 21]. As can be seen from Table 7, most of these transforms have been analyzed in reference to image processing. There is no one source that has an extensive list of transforms and the applications for which they provide the best results. The Karhunen–Loeve (KL) transform and Singular Value Decomposition (SVD) transforms give the best description of a signal in the least mean square error sense [20, 22]. However, they are used mainly for analyzing signals, because they have no fast algorithms like the Fourier transform. Faster and less accurate algorithms can be used with excellent results given the appropriate application.

The Hadamard, Walsh, Haar and Slant transforms are fast algorithms, but they have discrete value basis vectors [20, 23]. Therefore these transforms work well for square or step type signals. Because the pulse oximetry signal is sinusoidal in nature, transforms with sine and cosine basis vectors would appear to be a better choice.

Transforms with sine and cosine basis vectors include the Discrete Cosine Transform (DCT), Discrete Sine Transform (DST), Discrete Hartley Transform (DHT), and the Discrete Fourier Transform (DFT) or Fast Fourier Transform (FFT) [20, 24–27]. The DCT and DST can be interchanged by shifting the transforms by 90°, and should achieve similar results. The DFT uses both sine and cosine basis vectors. The DFT uses complex arithmetic, however, using these transforms provides both the magnitude and phase relationships of the signal. The DCT and DST magnitude and phase relationships are not directly interpreted, but the frequency resolution is twice as accurate as the DFT. The DCT and DST also do not require complex arithmetic. The DHT has sine and cosine basis vectors, but they are not interpreted as real and imaginary values. This interpretation results in no complex arithmetic, but like the DST and DST loses the magnitude and phase interpretation.

To identify which transform would work the best, the theoretical accuracy of these transforms was calculated [21] and for a detailed derivation refer to [28]. All three transforms are theoretically exact if the transform is performed on one period of the

Table 7. Basic time signal transforms

Transform	Applications used	Strengths/limitations
Karhunen–Loeve (KL)	Performance evaluation, performance bounds	Best mean square error energy, compaction for ensemble, no fast algorithm
Singular Value Decomposition (SVD)	Image restoration, power spectral estimation, data compression	Good energy compaction, no fast algorithm
Hadamard–Walsh	Image data compression, filtering, code design	Faster than sinusoidal transforms, no multiplications required, difficult to analyze
Haar	Feature extraction, image coding, image analysis	Very fast transform
Slant	Feature extraction, image coding	Fast transform, image like basis, good energy compaction
Fourier (DFT/FFT)	Signal processing, convolution, filtering	Complex arithmetic required, Good energy compaction
Cosine (DCT)	Transform coders, Weiner filters	Excellent energy compaction, Near optimal substitution for KL transform
Sine (DST)	Transform coders, Weiner filters	Very good energy compaction

Table 8. Fast algorithm computation requirements

Transform	Multiplications	Additions
SRFFT	$N(\log N-3)+4$	$3N(\log N-1)+4$
RSFFT	$N/2(\log N-3)+2$	$N/2(3\log N-5)+4$
DHT	$N/2(\log N-3)+2$	$3N/2\log N-(39N-12(-1)^{\log N})/18+4$
DCT	$N/2\log N+1$	$3N/2\log N-N+1$
DCT IV	$N/2\log N+N$	$3N/2\log N$

waveform. Each cycle falls on the sinc function zero crossing, and the error amplitude continues to decrease between each zero crossing. To evaluate the error expected, the interval from 4 to 5 periods was evaluated to identify the maximum error over the interval. The nominal time interval is about 4 s and 4–5 cardiac cycles would be expected. The error starts at zero and increases as it approaches one half period and then decreases uniformly back to zero. This is consistent with the sinc function. The maximum error at 4.5 cycles for a 0.5 amplitude signal is 0.039. This is a 7.8 per cent error which is significant. However, both the red and infrared signals will introduce the same error. Both signals are in phase and should therfore introduce the same error. When the R value is calculated, the error is eliminated and is given as

$$R=\left[\frac{AC_R/DC_R}{AC_{IR}/DC_{IR}}\right]\Rightarrow\left[\frac{AC_R*1.078/DC_R}{AC_{IR}*1.078/DC_{IR}}\right]=\left[\frac{1.078}{1.078}\right]\left[\frac{AC_R/DC_R}{AC_{IR}/DC_{IR}}\right]=R. \quad (5)$$

Although the error is theoretically reduced to zero, in practice some residual error will remain. Whether the residual error is significant is identified in processing and testing data.

In addition to accuracy, a comparison of computation requirements was performed. The formulas for the number of computations for specific optimized algorithms are listed in Table 8 and the formulas are evaluated for a number of transform sizes in Table 9 [21]. As can be seen, the real input split radix FST (RSFFT) and DHT use approximately the same number of multiplications and additions. The DCT algorithm, however, tends to use more computation than the RSFFT. Also the DCT uses fewer computations than the split radix FFT (SRFFT). Overall the fast implrmentations are similar in computation for small transforms and does not provide a clear choice for which algorithm is the best. A mean square output for each of the transforms is shown in Figs 6 and 7. There are many other basic transforms that have been used. Most of these transforms are similar to the transforms described, and each with minor differences in performance. Therefore several transforms were selected for testing.

Selected transforms

The FFT originally considered for improving pulse oximetry measurements, transforms the time domain signal into the frequency domain. The FFT is a fast and efficient

Table 9. Fast algorithm computation evaluation

	SR FFT		RS FFT		DH T		DC T		DCT IV	
N	Mult.	Add	Mult.	Add	Mult.	Add	Mult.	Add	Mult.	Add
8	4	52	2	20	2	22	13	29	20	36
16	20	148	10	60	10	66	33	81	48	96
32	68	388	34	164	34	174	81	209	112	240
64	196	964	98	420	98	442	193	513	256	576
128	516	2308	258	1028	258	1070	449	1217	576	1344
256	1284	5380	642	2436	642	2522	1025	2817	1280	3072
512	3076	12292	1538	5636	1538	5806	2305	6401	2816	6912
1024	7172	27,652	3586	12,804	3586	13,146	5121	14,337	6144	15,360
2048	16,388	61,444	8194	28,676	8194	29,358	11,265	31,745	13,312	33,792

algorithm for computing the DFT. The cardiac signal of interest is a sinusoidal signal and is represented in the FFT as a single spectral line. Because the pulse oximetry plethysmogram signal is sinsoidal in nature, the best analysis tools to consider would be transforms with sinusoidal basis vectors. The FFT was used with plethysmogram data to calculate SpO_2 values with good results, since it uses sine and cosine basis vectors. The FFT was selected for further testing of SpO_2 computation. The DCT and DST appeared to be a natural selection also, because they have sinusoidal basis vectors. The DST can be derived from the DCT using a 90° phase shift and should provide comparable results. Therefore the DCT was selected for further testing. Both transforms provide the same theoretical accuracy and provide similar computation complexity.

Transform optimization

Before any alternate transforms were identified, the preliminary work focused on identifying the best FFT format to process the digital photoplethysmogram (DPP) data. When processing the transform, the FFT size determines how fast and how much memory is required. Therefore one of the objectives in the analysis was to identify the minimum size FFT needed to provide acceptable results. Other factors influencing the transform are the sample rate and processing time interval. A sample frequency too slow would not provide enough resolution. The time interval is restricted from being too long or too short. If the DPP data time interval is too long, then the assumption of stationarity is not valid, which the Fourier transform requires. If the time interval is too short then not enough cardiac cycles would be present to calculate an accurate cardiac amplitude.

Many of the trends presented in Tables 2 and 3 were expected. As discussed earlier, the FFT is based on stationarity and the longer time intervals would expect to become worse, as is noted in Table 2. At a sample frequency of 60 Hz and using 2048 points over a 34.13 s time interval, a bias of -2.73 and a precision of 10.15 was calculated. This is worse than the bias of 0.54 and precision of 3.73 for the 240 Hz, 1024 point bench mark. As the time interval decreases, accuracy problems arise. If the time interval is not one period or an exact mutliple of the cardiac period, the transform will not accurately identify the amplitude. Below one period, the error is almost 100 per cent. Therefore a longer time interval with more cardiac cycles would reduce transform error. In addition to accuracy, as fewer points are used, the resolution decreases until the cardiac rate can no longer be distinguished. The lose of resolution is present in the frequency plot shown in Fig. 8. The decimated time signal no longer represents the DPP signal, and the cardiac spectral line is lost in the DC component and THM frequencies. Also note the highest frequency resolved is at 1.6 Hz. If a fast cardiac rate is encountered the AC component would be missed completely by the transform. These results were used to narrow the ranges used for further analysis. The number of samples was reduced to 32, 64 and 128 points, and the frequency range was reduced to 7.5, 15 and 30 Hz. Tables 2 and 3 indicate that the FFT provided acceptable results at a sample rate of 15 Hz and using a 64 point transform size.

Overall the DCT and FFT performed well. One interesting fact is the DCT performed better for some regions while the FFT performed better in other regions. This could be attributed to the fact that the DCT uses only cosine basis vectors and has twice the frequency resolution of the FFT, while the FFT uses both sine and cosine basis vectors. After reviewing the data, there were obvious locations in the data sets that produced most of the errors. There was an attempt made to identify if some form of averaging or eliminating points would improve the results.

The frequencies shown in Fig. 9 include the DC component and THM frequencies, AC cardiac amplitude with harmonics, noise and distortion. The DC component and AC cardiac frequency are the desired frequencies. The THM frequencies result from the automatic nervous system and range from 0.07 to 0.5 Hz [29,30]. The THM frequencies can easily be isolated by using enough resolution. The harmonics, noise and distortion appear at frequencies higher than the cardiac rate and can also easily be isolated.

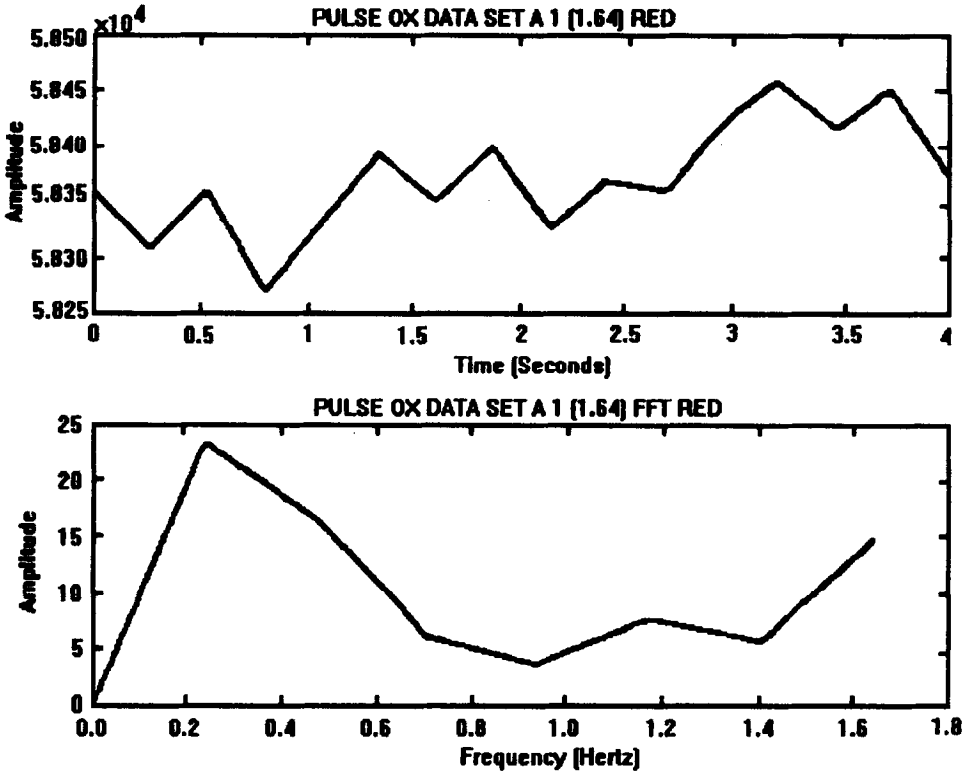

Fig.8. Loss of resolution at a sample rate of 7.5 Hz.

Advanced transforms

The search for alternate transforms was more extensive than the basic transforms discussed. Advanced transforms were also identified. A category of transforms currently being applied in many areas is a combined time and frequency transform. Advanced transform techniques include lapped transforms and wavelet transforms.

Lapped transforms are being applied in filtering applications. As the name implies, the lapped transform uses a window that is overlapped in time [31]. In standard windowing, each window has a unique set of data, and as a result when the signal is recreated there is a discontinuity at each window. In lapped transforms, the windows are overlapped at each end and when the signal is recreated, there is much less discontinuity at the window boundaries. The technique is designed to minimize additional processing when compared to its non-overlapped counterpart. Various transform basis vectors have been used, but

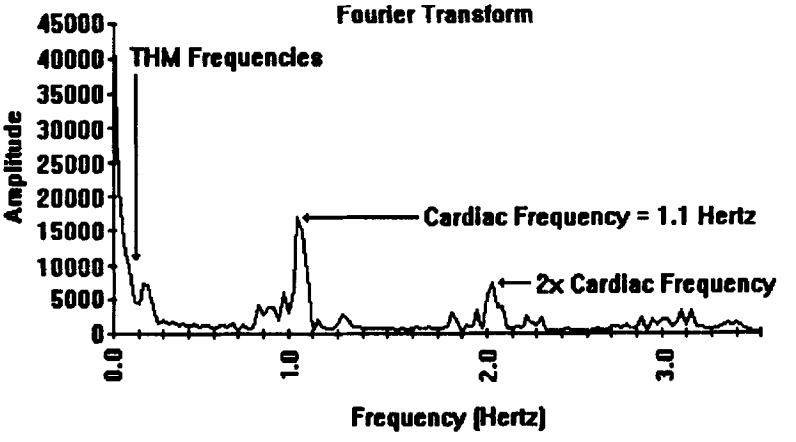

Fig. 9. Cardiac spectral line.

Table 10. Comparison of pulse oximetry bias and precision

Algorithm	Bias	Precision	Reference
WMA	±1.7%	2.4%	Ohmeda 3700 Manual, 1988
WMA	5.5%	4.2%	[34]
WMA	0.2%	7.6%	[35]
WMA	13.1%	5–16%	[36]
WMA	2.6%	1.5–2.8%	[37]
DHT	−0.1%	4.3%	See methods
FFT	−0.2%	2.9%	See methods
DCT	0.4%	1.7%	See methods

the lapped transform based on the DCT is one of the more common examples. Although the lapped transform may be ideal for signal filtering, manipulation and reconstruction, it does not provide much incentive for being applied to pulse oximetry. For pulse oximetry the signal is not recreated and boundary discontinuity is not a problem.

Wavelet transforms are very impressive because they represent both the time and frequency aspects of a signal [32–33]. Wavelets have become very important in image processing and compression techniques. Using both the time and frequency is extremely important if a signal is time varying, which includes the pulse oximetry signal. Wavelets therefore appear to be a possible solution for improving pulse oximetry measurements. The disadvantage with wavelet transforms can be the amount of processing required and the interpretation of the results. An in-depth analysis of wavelet transforms applied to pulse oximetry is a research project by itself, and was not pursued in detail for this paper.

CONCLUSION

This research was an attempt to improve on current pulse oximetry algorithms. In addition other alternate transforms such as the wavelet transform were studied. Two transforms, the FFT and DCT were selected and tested for SpO_2 computation.

There are several contributions that this research provided. The first contribution was to show the use of spectral analysis to calculate oxygen saturation (SpO_2) values is a practical solution. This was accomplished by processing archived DPP data. Enough evidence was present to implement a stand alone design which could prove the use of spectral analysis for portable pulse oximetry. The second was to identify alternate methods of computing the SpO_2 values that provided acceptable results. Both the FFT and DCT proved acceptable. Further testing on additional data sets is required to show if one is superior to the other. However, at this time, both appear to provide similar results.

The information gathered and designs developed during the course of this research have been very encouraging. Two transforms, the FFT and DCT, were identified as possible improvements to current pulse oximeters. The tests performed with the FFT and DCT were not conclusive, but show the potential for accuracy and improved response. The FFT has the potential to improve accuracy, because the cardiac frequency can more easily be isolated. Motion artifact produces low frequency components. In general these low frequencies are automatically separated from the cardiac frequency. Another related problem, shivering could easily be isolated from the cardiac frequency. Shivering can be a problem in cool operating room environments.

The test data processed with the FFT and DCT, with no attempt to average data or otherwise improve results, was as good or better than current pulse oximeters on the market. A comparison to current pulse oximeters is listed in Table 10. The computed SpO_2 data are compared to various sources. The first source was taken from a pulse oximeter users manual on expected accuracy and the remaining sources are from research studies of pulse oximeters.

There are three clear directions that can be pursued from this research. The first is additional testing of wavelet transforms for SpO_2 computation. Wavelet transforms

require careful analysis, because the cardiac amplitude is not directly apparent from the transform. The FFT results in a unique frequency with the amplitude directly available. The wavelet transform does not always identify a unique value for the cardiac frequency. However, the diversity of the wavelet transform may provide a means to greatly improve SpO_2 computation oximetry calculations. It would therefore be beneficial to perform a diverse test of wavelet transforms in an effort to identify an improved algorithm.

A second direction is testing of the current pulse oximetry prototype. Some changes and formal testing is required to guarantee the successful implementation of the FFT pulse oximeter. Also testing the pulse oximeter and improving the calculations to reduce or eliminate motion artifact is needed. Further testing can identify inaccuracies during low perfusion or errors during motion artifact. Averaging of data and elimination of invalid SpO_2 values could be implemented with the prototype to correct for these errors.

The final decision in implementing a portable pulse oximeter is to complete a very large scale integration (VLSI) design. After the design is verified and the processing algorithm is finalized, a single chip implementation of the pulse oximeter could be achieved. A VLSI implementation would yield a miniature, power efficient, and reliable pulse oximeter. Having such a unit would provide an affordable unit which could be used for numerous applications, which are currently not feasible. If cost was reduced, the pulse oximeter could be used in standard monitoring of humans in adverse conditions. This could save the lives of miners, firefighters, divers, and others by providing continuous monitoring and indicating when a person has reached their physical limits.

REFERENCES

1. J. W. Severinghaus and P. B. Astrup, History of blood gas analysis, *Int Anesthesiology Clinics* **25** (1987).
2. J. W. Severinghaus and J. F. Kelleher, Recent developments in pulse oximetry, *Anesthesiology* **76,** 1019–1038 (1992).
3. J. T. Moller, N. W. Johannessen, K. Espersen, O. Ravio, B. D. Pedersen, P. F. Jensen, N. H. Rasmussen, L. S. Rasmussen, T. Pedersen, J. B. Cooper, J. S. Gravenstein, C. Chraemmer-Jorgensen, M. Djernes, F. Wilberg-Jorgensen, L. Heslet and S. H. Johansen, Randomized evaluation of pulse oximetry in 20,802 patients: II, *Anesthesiology* **78,** 445–453 (1993).
4. E. H. Wood and J. E. Geraci, Photoelectric determination of arterial oxygen saturation in man (1943).
5. F. W. Cheney, The ASA closed claims study after the pulse oximeter, *ASA Newsletter* **54,** (1990).
6. J. A. Pologe, Pulse oximetry: Technical aspects of machine design, *Int Anesthesiology Clinics* **25,** (1987).
7. K. K. Tremper and S. J. Baker, Pulse oximetry and oxygen transform, *Pulse Oximetry,* Ch 3, Springer-Verlag, Berlin (1986).
8. J. A. H. Bos, W. Schelter, W. Gumbrecht, B. Montag, E. P. Eijking, S. Armbruster, W. Erdmann and B. Lachmann, Development of a micro transmission cell for in vivo measurements of SaO_2 and Hb, *Oxygen Transport to Tissue XII,* pp. 47–53. Plenum Press, New York.
9. K. K. Tremper and S. J. Baker, Pulse oximetry: applications in *Advances in Oxygen Monitoring.* Springer-Verlag, Berlin (1987).
10. J. C. S. Lee, P. W. Cheung, D. R. Marble, M. A. Kenny and D. Landicho, Measurement of percent carboxyhemoglobin with pulse oximetry technique, *Proc 10th Annual International Conference of the IEEE Engineering in Medicine and Biology Society,* 1781–1782 (1988).
11. J. C. S. Lee, P. W. Cheung, D. R. Marble, M. A. Kenny and D. Landicho, Simultaneous measurement of percent carboxyhemoglobin and functional oxygen saturation, *Proc 11th Annual International Conference of the IEEE Engineering in Medicine & Biology Society,* 1092–1093 (1989).
12. M. R. Neuman and W. Wang. Motion artifact in pulse oximetry, *Proc 12th Annual International Conference of the IEEE Engineering in Medicine and Biology Society* **12,** 2007–2008 (1990).
13. L. K. L. Lum and P. W. Cheung, A controlled motion artifact study of EKG synchronization on pulse oximetry, *Proc. 12th Annual International Conference of the IEEE Engineering in Medicine and Biology Society* **12,** 2009–2011 (1990).
14. L. K. L. Lum and P. W. Cheung, Evaluation of pulse oximetry with EKG synchronization, *Proc. 10th Annual International Conference of the IEEE Engineering in Medicine and Biology Society* 1223–1224 (1988).
15. J. E. Scharf, S. Athan and D. Cain, Pulse oximetry through spectral analysis, *Proc. of the Twelfth Southern Biomedical Engineering Conference* (1993).
16. G. B. Drummond and G. R. Park, Arterial oxygen saturation before intubation of the trachea, *Brit. J. Anaesthesia* **56,** 987–982 (1984).
17. M. L. Heller and T. R. Watson, Polarographic study of arterial oxygenation during apnea in man, *The New England J. Medicine* **264** (1961).
18. S. W. Weitzner, B. D. King and E. Ikezono, The rate of arterial oxygen saturation during apnea in humans, *Anesthesiology* **20,** (1959).
19. J. E. Scharf and T. L. Rusch, Optimization of portable pulse oximetry through Fourier analysis, *Proc. of the Twelfth Southern Biomedical Engineering Conference,* 233–235 (1993).
20. A. K. Jain, *Fundamentals of Digital Image Processing.* Prentice Hall, New Jersey (1989).

21. D. F. Elliot and K. R. Rao, *Fast Transforms: Algorithms, Analysis, Applications*. Academic Press, New York (1982).
22. V. U. Reddy and L. S. Biradar, SVD-based information theoretic criteria for detection of the number of damped/undamped sinusoids and their performance analysis, *IEEE Trans. Signal Processing* **41**, 2872–2881 (1993).
23. L. W. Chang and M. C. Wu, A bit level systolic array for Walsh–Hadamard transforms, *Signal Processing* **31**, 341–343 (1993).
24. B. Lee, A new algorithm to compute the discrete cosine transform, *IEEE Transactions on Acoustics, Speech, and Signal Processing* **32**, 1243–1245 (1984).
25. Z. Wang, Fast discrete sine transform algorithms, *Signal Processing* **19**, 91–102 (1990).
26. M. A. O'Neil, Faster than fast Fourier, *Byte Magazine*, 293–300 (1988).
27. A. V. Oppenheim and R. W. Shafer, *Discrete-Time Signal Processing*. Prentice Hall, New Jersey (1989).
28. J. T. Rusch, *Implementation and design of a portable pulse oximeter using spectral analysis*, M.S. Thesis, University of South Florida, Tampa, Florida (1994).
29. M. Pagani, F. Lombardi, S. Guzzetti, O. Rimoldi, F. Furlan, P. Pizzinelli, G. Sandrone, G. Malfatto, A. Dell 'Orto, E. Piccaluga, M. Turiel, G. Baselli, S. Cerutti and A. Malliani, Power spectral analysis of heart rate and arterial pressure variabilities as a marker of sympatho-vagal interaction in man and conscious dog, *Circul. Res.* **59**, 178–193 (1986).
30. T.L. Rusch, J. E. Scharf and R. Sankar, Alternate pulse oximetry algorithms for SpO_2 computation, *Proc. 16th Annual International Conference of the IEEE Engineering in Medicine and Biology Society* (1994).
31. H. S. Malvar, *Signal Processing with Lapped Transforms*. Artech House, Boston (1992).
32. D. E. Newland, *An Introduction to Random Vibrations, Spectral and Wavelet Analysis* Ch. 17. John Wiley, New York (1993).
33. O. Rioul and M. Vetterli, Wavlet and signal processing, *IEEE Signal Processing Magazine* **10** (1991).
34. M. J. Sendak, A. P. Harris and R. T. Donham, Accuracy of pulse oximetry during arterial oxyhemoglobin desaturation in dogs, *Anesthesiology* **68**, (1988).
35. S. Lee, K. K. Tremper and S. J. Barker, Effects of anemia on pulse oximetry and continuous mixed venous hemoglobin saturation monitoring in dogs, *Anesthesiology* **75**, 118 (1991).
36. J. W. Severinghaus and K. H. Naifeh, Accuracy of six pulse oximeters to profound hypoxia, *Anesthesiology* **67**, (1987).
37. S. Takatani, C. Davies, N. Sakakibara, A. Zurick, E. Kraenzler, L. R. Golding, G. P. Noon, Y. Nose and M. E. DeBakery, Experimental and clinical evaluation of a noninvasive reflectance pulse oximetry sensor, *J. Clin. Monit.* **8**, (1992).

About the Author—TERRY L. RUSCH received his BSEE from the University of Wisconsin Madison in 1986 and MSEE from the University of South Florida in 1994. He is currently Senior Genomics Engineer at the Marshfield Medical Research Foundation, Marshfield, Wisconsin, where he is responsible for the design, test, and maintenance of genetic scanning fluorescence detector (SCAFUD) instrumentation. He was with Group Technologies Corporation in Tampa, Florida, in 1994 and was Vice President/Manager of Research and Development in Vibration Consultants, Inc., Tampa, Florida from 1987 to 1992.

His current research interests include genetic analysis and sequencing using flourescence scanning, and biomedical instrumentation and design. He is a member of IEEE, member of IEEE Signal Processing Society and Engineering in Medicine and Biology Society.

About the Author—RAVI SANKAR received the B.E. (Honors) degree in Electronics and Communication Enginerring from the University of Madras, India, the M.Eng. degree in Electrical Engineering from Concordia University, and the Ph.D. degree in Electrical Engineering from the Pennsylvania State University. Since 1985, he has been with the Department of Electrical Engineering at the University of South Florida, Tampa, where he is currently an Associate Professor.

His research interests are in the areas of Communication/Computer Networking, Wireless Communication Networks, Signal Processing and its Applications, Speech Processing and Recognition, Applications of Neural Networks and Fuzzy Logic, Simulation and Modelling. He has conducted successful research projects and has published widely in these areas.

He is a Senior Member of IEEE, member of IEEE Communications Society, Computer Society, Signal Processing Society, IEEE Communication Society Technical Comittee on Computer Communications. He is also a Registered Professional Engineer in the State of Florida. He currently serves as the Technical Program Chair for IEEE Southeastcon '96 and the Vice-Chair for IEEE Signal Processing Society Chapter of the Florida West Coast Section. He co-guest edited a special issue of SIMULATION magazine on Simulation of Communication-Computer Networks published in February 1992. He is a reviewer for IEEE Project 802.x draft proposals (standards) and a referee for several journals and conferences.

About the Author—JOHN E. SCHARF, MD is an Assistant Professor of Anesthesiology at the University of South Florida. He specializes in the management of critically ill patients during the peri-operative period at James A. Haley Veterans' Hospital in Tampa. His research interests are in non-invasive biomedical engineering projects. Currently, specialized interest is focused upon the digital signal processing and spectral analysis of skin blood flow waveforms. This focus includes the acquisition, processing, and display of pulse plethysmograms with a portable, miniature, wireless, open-architecture device.